Journal of the European Ceramic Society **18** (1998) 1001–1009

PII: S0955-2219(97)00193-3
0955-2219/98/$19.00 + 0.00

Finite Element Modelling of Binder Removal from Ceramic Mouldings

Andrey Maximenko and Omer Van Der Biest*

Katholieke Universiteit Leuven, Departement Metaalkunde en Toegepaste Materiaalkunde, de Croylaan 2, B-3001 Leuven (Heverlee), Belgium

(Received 28 July 1997; accepted 7 November 1997)

Abstract

The article is devoted to the numerical simulation of the thermal debinding process during powder injection moulding. The model of the binder removal incorporates both main transport mechanisms during debinding, namely, the diffusion of the low molecular weight component and the forced or capillar flow of the binder. Optimization of the heating regimes is proposed to be based on the prediction of the internal stress distribution in the workpiece. Internal pressure is induced by the swelling of the binder during thermal degradation of the polymer or its shrinkage, accompanying the loss of the low molecular weight component. Calculations were accomplished for poly-alphamethylstyrene as organic vehicle for which sufficient data are available. The stress distribution and damage conditions were assessed in the case of a cylindrical and a slab shaped workpiece. The results of the modelling correspond well with experimental data. They confirm that damage during thermal debinding can be explained as a result of the development of internal stresses due to imbalance between degradation of the polymer and outward transportation of resulting products. © *1998 Elsevier Science Limited. All rights reserved*

Keywords: (A) Injection moulding, (B) Failure analysis, (C) Diffusion, Mechanical properties, (D) Traditional ceramics

1 Introduction

Powder injection moulding is a widespread method for the production of complex-shaped parts from ceramic or metallic powders. The salient feature of the process is a dispersing of the powder into polymeric vehicle to increase moldability of the powder assembly and strength of the greenware after cooling. The binder removal after the moulding is one of the most critical steps in this process. It takes the major part of the processing time and if one attempts to accelerate debinding it often results in failure of the powder compact.

The most simple and principally the most viable method of binder removal for mass production is thermal debinding. In the course of the process the binder is burned out by the controlled heating of the part. The conventional drawback of thermal debinding is the high risk of defect formation or even total destruction of the ceramic mouldings in the case of an inappropriate heating regime. The theoretical modeling allows optimization of the present technological operation schedules and suggests new ways for the development of technologies.

The binder removal is always an interplay of different physical processes. The main specific features of thermal debinding are heating of the workpiece, mass transport of the binder in the powder skeleton and active chemical reactions at high temperatures. Disparate transport mechanisms differ in their physical origins of binder flow. In many cases the liquid binder is driven to the surface of the part by capillary pressure or any other pressure gradients.[1] Diffusion of the low molecular weight constituents of the binder is generally not taken into account. But it was shown,[2,3] that diffusion can be the main transport mechanism at low temperatures.

The next important feature of thermal debinding is that the use of a high molecular weight polymer necessitates its decomposition to provide removal of the polymer. One of the most likely causes of damage during thermal debinding of powder compacts with a polymer vehicle is an imbalance between degradation of the polymer in a volume of the part and the outward transportation of the resulting products of decomposition.

*To whom correspondence should be addressed. Fax: 016 321 992; e-mail: Omer.VanDerBiest@mtm.kuleuven.ac.be

The present investigation takes into consideration both fundamental transport processes during debinding and an impact of the decomposition rate on the binder flow. The internal stress distribution in the part is calculated and a damage criterion proposed. The results will be compared with experimental data published in.[3]

2 Mathematical Model of the Transport Processes

A general mathematical formalism for the transport processes in porous media can be presented in the form of the generalized Stefan-Maxwell equations:[4]

$$(\mathrm{grad}\mu_1)_T = \frac{x_2}{a_{12}}(\mathrm{v}_2 - \mathrm{v}_1) + \frac{1}{a_{1s}}(\mathrm{v}_s - \mathrm{v}_1) \qquad (1)$$

$$(\mathrm{grad}\mu)_T = \frac{x_1}{a_{21}}(\mathrm{v}_1 - \mathrm{v}_2) + \frac{1}{a_{2s}}(\mathrm{v}_s - \mathrm{v}_2) \qquad (2)$$

where a_{ij} and a_{is} are some phenomenological parameters obeying the symmetry conditions

$$a_{ij} = a_{ji}$$

v_s is the velocity of the powder skeleton and v_i, x_i are velocities and molar fractions of the binder components, respectively. All velocities are taken in the laboratory frame of reference. The number of chemical potentials μ_i corresponds to the number of binder components. We shall only concentrate on a two-component binder. One component is the low molecular weight one or LMWC and the other is the high molecular weight component or HMWC. LMWC is the product of degradation of HMWC or is due to initial wax constituent of the binder. The subscript 1 will be always affixed to the parameters of LMWC.

Having regard that thermal debinding is a rather slow process and it is usually used for manufacture of small parts, we shall ignore thermal gradients and consider a uniform temperature as a given function of time.[1]

It was experimentally proven,[2] that the mass flux of LMWC does not depend on the powder particle average size and permeability of the powder compact. Consequently, we can neglect the term with $\mathrm{v}_s - \mathrm{v}_1$ in the right-hand part of (1). Next assumption is that diffusion of LMWC in HMWC is a quasi-static process and the Gibbs–Duhem equation for the chemical potentials is valid:

$$c_1(\mathrm{grad}\mu_1)_{T,P} + c_2(\mathrm{grad}\mu_2)_{T,P} = 0 \qquad (3)$$

where c_1, c_2 are molar volume concentrations of the components. When pressure gradients are present, the calculations of the same combinations of potentials with due regard for (1), (2) give the following result:

$$\mathrm{grad}P = \frac{c_2}{a_{2s}}(\mathrm{v}_s - \mathrm{v}_2) \qquad (4)$$

Equations (1) and (2) [or eqns (1) and (4)] are the constitutive relationships of the transport processes in the powder compact. They allow determination of the velocities at any moment of time if pressure and composition of the binder are known. In turn, the correlations between velocities and densities of the components are given by the equations of mass conservation:

$$\partial(\varepsilon_i\rho_i)/\partial t + \mathrm{div}(\rho_i\mathrm{v}_i) = m_i \qquad i = \overline{1,2} \qquad (5)$$

where ε_i are the volume fractions of the components and m_i is the rate of mass production per unit volume. In our case the origin of mass production is thermal decomposition of polymer at high temperature. For the complete mathematical statement of the problem it is necessary to specify chemical potentials as functions of the component concentrations and subject all equations to the boundary and initial conditions of the flow.

3 Extremum Statement of the Problem

The use of the finite element method for the modelling calls for some extrmum statement of the problem. For the constitutive eqns like (1),(4) it is possible to utilize the extremum principles of irreversible thermodynamics. The formalism of this approach is founded on the determination of fluxes J_i and forces X_i driving the ith process.[5] Let us define

$$\begin{aligned} J_1 &= \rho_1(\mathrm{v}_1 - \mathrm{v}_2);\ X_1 = -(\mathrm{grad}\mu_1)_T \\ J_2 &= \rho(\mathrm{v}_2 - \mathrm{v}_s);\ X_2 = -\mathrm{grad}P \end{aligned} \qquad (6)$$

New notations impart the common simple form to eqns (1) and (4)

$$X_i = \frac{J_i}{a_i} \qquad i = \overline{1,2} \qquad (7)$$

where a_1, a_2 are some phenomenological coefficients which can be determined contrasting eqn (7) against the known relationships for the transport processes. Equations (6) or (7) describe all transport mechanisms including forced or capillary flow

of the binder as a whole as well as diffusion of LMWC in the binder.

If we determine dissipative potential Φ as follows:

$$\Phi = \frac{1}{2}\sum_{1}^{N} X_i(J_1, \ldots, J_N)J_i \tag{8}$$

the real fluxes of the process render stationary value for the functional[6]

$$F = \int_{\Omega}(\Phi - \sum_{1}^{N} X_i J_i)\mathrm{d}\Omega \tag{9}$$

where X_i must be treated as given values. Ω,S denote the volume and the surface of the workpiece at hand. The similar functional can be derived in terms of unknown forces provided fluxes are considered as known ones. In our case the functional (9) is the sum of the two functionals

$$F_1 = \int_{\Omega}\left[\frac{1}{2}a_1 X_1^2 - \mu_1 \mathrm{div}(J_1)\right]\mathrm{d}\Omega + \int_{s}\mu_1(J_1 \cdot n)\mathrm{d}S \tag{10}$$

$$F_2 = \int_{\Omega}\left[\frac{J_2^2}{2a_2} - P\mathrm{div}(J_2)\right]\mathrm{d}\Omega + \int_{s}P(J_2 \cdot n)\mathrm{d}S \tag{11}$$

The functionals (10),(11) were deduced from (9) by substitution (1),(4) and proper use of some simple integral transformations. Parameters X_1 in (10) and J_2 in (11) are unknown and J_1, P should be considered as given functions. Functional (11) does not contain unknown parameters of diffusion process, thus it can be minimized independently. Functional (10) according to (6) depends on the velocity of LMWC in the framework of the binder. The flux J_1, which is treated as a given parameter in the ensuing transformations will be replaced by its representation from (5).

Equation (4) can be treated as Darcy's law and in this case parameter a_2 assumes the following form:

$$a_2 = K\rho/\mu \tag{12}$$

where K is the permeability of the powder bed[1] and μ is the viscosity of the binder. For the permeability K the following approximation was used[7]

$$K = 4{\cdot}8 \times 10^{-13}\mathrm{d}^{1{\cdot}3}(1 - \varepsilon_s)^{4{\cdot}8} \tag{13}$$

where d is the average diameter of powder particles in μm if K has dimensions of m^2, ε_s is the powder loading.

It should be noted that eqn (4) describes the flow of HMWC relative to the velocity of the skeleton. This means that swelling or shrinking of the polymer combined with the same deformation of the skeleton cannot be predicted from (1) and they will be determined through additional conditions.

If influence of pressure gradients on the diffusion is neglected, the functional (10) can be rewritten in the more convenient form with respect to the weight fraction y_1 of LMWC in the binder:

$$F_1 = \int_{\Omega}\left[\frac{1}{2}D_y(\mathrm{grad}(y_1))^2 + \Delta y_1\left(\frac{\rho}{2}\frac{\Delta y_1}{\Delta t} - m_1\right)\right]\mathrm{d}\Omega - \int_{s} D_y y_1 \frac{\partial y_1}{\partial n}\mathrm{d}S \tag{14}$$

where

$$D_y = D\rho(1 + \rho_1(V_2 - V_1))$$
$$\Delta y = y_1(t) - y_1(t - \Delta t)$$

D is the diffusion coefficient of LMWC in the binder, Δt is the time increment and $y_1(t - \Delta t)$ is the weight fraction at the previous step of calculations. The time derivative of y_1 is taken in the framework of HMWC. The relationship (14) follows from (10) after substitution (6) and (5) where X_1 is considered as a function of concentration. The use of (14) is similar to utilization of the implicit finite difference approaches in the theory of differential equations. Minimization of (14) allows determination step by step of the weight fraction of LMWC at any moment of time.

The boundary conditions for (14) assumes an adequate sweep of gas and zero surface concentration of LMWC at the boundary of the workpiece

$$y_1 = 0 \text{ at } S \tag{15}$$

After substitution (12),(6) functional F_2 assumes the form

$$F_2 = \int_{\Omega}\left[\mu/2K\,(\mathrm{v}_2 - \mathrm{v}_s)^2 - P\mathrm{div}(\mathrm{v}_2 - \mathrm{v}_s)\right]\mathrm{d}\Omega - \int_{s} P(\mathrm{v}_2 - \mathrm{v}_s) \cdot n\mathrm{d}S \tag{16}$$

For the correct assessment of pressure P it is necessary to take into account all origins of internal stresses in the powder compact. First of all stresses arise due to inhomogeneous volume change in the

workpiece during debinding. Such stresses are completely similar to the so-called 'thermal stresses', which appear during non-uniform heating of elastic body.[8] To predict the stresses we must know the elastic moduli of the powder compact as a whole and the volume change in the course of debinding. The powder compact saturated with binder has a large bulk elastic modulus due to poor compressibility of liquid polymer. The bulk modulus K_p for the polystyrene was calculated through the Tait-relation[9] and is given in the Appendix. The effective bulk modulus of the powder–binder mixture was calculated through simple additive rule:

$$K_E = \varepsilon_s K_s + (1 - \varepsilon_s) K_p \tag{17}$$

where ε_s and K_s are the powder loading and bulk modulus of the powder skeleton. The shear modulus of the powder compact was assumed equal to the shear modulus of powder skeleton G_s. Elastic constants for the skeleton were taken from Ref. 10 and they can also be found in the Appendix.

The local volume change of the compact is a result of swelling or shrinkage of the binder. In the course of thermal degradation the LMWC products of depolymerization have a higher specific volume than the initial polymer. Consequently, such process must lead to swelling of the binder. In the calculations no volume contraction was supposed to accompany the mixing of LMWC and HMWC. The contribution of volume shrinkage during mixing can be taken into consideration with the use of cumbersome calculations (see, for example, Ref. 11 for polystyrene and ethylene), but influence of this adjustment is negligible in comparison with the precision of available experimental data.

Shrinkage of binder results from decrease of LMWC due to its outward diffusion. Note that shrinkage is non-uniform in the volume of the part and it always produces internal stresses.

In general, the extra volume deformation can be assessed from the following relationship:

$$\frac{\mathrm{d}\delta}{\mathrm{d}t} = \rho V_1 \frac{\mathrm{d}y_1}{\mathrm{d}t} - V_2 m_1 + e_c \tag{18}$$

where the first term in the right-hand part of (18) is the volume strain due to the change of LMWC concentration, the second term is the deformation due to decrease of the polymer volume and the last term is the rate of internal strain relaxation due to the flow of the binder:

$$e_c = -\mathrm{div}(\mathrm{v}_2) \tag{19}$$

For the calculations of LMWC mass production rate m_1 the equation for the kinetics of thermal degradation was taken from Ref. 3. It is given in the Appendix.

After determination of elastic moduli and volume changes the procedure of stress determination comes down to solving the equations of elasticity of powder compact under influence of the internal pressure $K_E\delta$. It should be noted, that in spite of the presence of the bulk modulus in the calculations, stresses due to inhomogeneous shrinkage are of the order of $G\delta'$, where $\delta' = \delta - \bar{\delta}$ and $\bar{\delta}$ is the volume averaged volume change.[8] We shall denote the contribution of stresses due to volume change to the internal pressure as P_T.

The next origin of internal stresses is the particle interaction in the course of deformation. They are due to the local mismatch between powder skeleton and binder displacements and depend on the properties of the powder skeleton. Generally, the skeleton exhibits viscoelastic properties. The usual assumption is that strain rate satisfies a Maxwell model:

$$\dot{\delta} = \frac{\dot{P}_s}{K_s} + \frac{P_s}{\eta_s} \tag{20}$$

where K_s is the bulk elastic modulus and η_s is the bulk viscosity of the skeleton and P_s is the pressure, which arises in powder compact. Above equation and utilization of the Frankel–Acrivos approach[12] for the viscous and elastic properties of the densely packed suspension leads to the following formula for the pressure:

$$P_s = \int_0^t K_s \dot{\delta} \exp\left(\frac{G_P}{\mu}(x - t)\right) \mathrm{d}x \tag{21}$$

where G_P, μ are shear elastic modulus and viscosity of the binder. The total pressure is a sum of the two terms:

$$P = P_T + P_s \tag{22}$$

Boundary condition for (16) was

$$P = P_{\mathrm{out}} - P_c \text{ at } S \tag{23}$$

where P_{out} is the ambient pressure. P_c is the capillary pressure, which was calculated in the form:[13]

$$P_c = \frac{9.6\sigma}{\mathrm{d}} \tag{24}$$

where d is the average particle diameter.

4 Criterion of Defect Formation

The optimization of the debinding process is impossible without some criterion of the 'bad' technological regime. In Refs 3 and 14 a new fracture criterion for the specimen during debinding was put forward. The criterion is based on the prediction of maximum vapour pressure in the volume of the powder compact. The condition is similar to the condition of boiling for liquids and it is assumed that if vapour pressure becomes greater than external one, the active bubble formation leads to the destruction of the workpiece. In our notations it is

$$P_v > P_{\text{out}} \tag{25}$$

Condition (25) had some experimental support.[3,14] It should be noted, that (25) does not depend on the presence of powder in the binder and the fracture process is completely determined by the properties of the binder.[3] This can give a reasonable first approximation. However if cracking of compacts during debinding is to be properly accounted for, then the properties of the powder–binder mixture as a whole need to be considered. This is also done in the theory of drying,[15] a process very similar to debinding.

In order to combine both approaches, we shall assume that cracking or bloating of the powder compact are really the result of cavitation, but cavitation manifests itself visibly only if it is accompanied by some dilatancy of the powder compact. This assumption is supported by the fact that considerable internal close porosity associated with 'boiling' of the binder was never observed in the powder compacts either during debinding or during drying without skeleton deformation.

In particulate materials dilatancy can be observed even in the case of compressive loading. Dilation of powder occurs in response to the deviatory strains. If the particles are densely packed, they must move into a looser configuration for deformation to take place.[16] As a condition of dilatant particle rearrangement we shall use the Drucker–Prager approximation of the Mohr–Coulomb friction criterion, which relates the shear stress τ_N along some plane in the powder compact to the stress σ_N normal to the plane and the adhesive force σ_0 between particles.[16]

$$\tau_N = \sigma_0 + \sigma_N \tan\varphi \tag{26}$$

where φ is the friction angle. Deformation of the particulate material occurs if the above equality is satisfied for some plane. In the Drucker–Prager approximation stresses are replaced by the corresponding invariants of the stress tensor. We shall use this condition in the form

$$\frac{\tau}{\tan\varphi} = P_0 + I_1/3 \tag{27}$$

The first invariant I_1 of stress tensor was taken positive for compressive stresses. The friction angle of powder medium depends on the type of particle packing and friction conditions between particles. In experiments with SiC particles (2 to 5μm) the friction angle was obtained equal to 18°.[17] We shall use this value for the assessments. The pressure $-P_0$ is the pressure, which will dilate the powdered material in the absence of shear stresses. This parameter characterizes the strength of powder compact. If condition (27) is met at some element of the powder compact, the irreversible deformation of the element becomes possible.

The second condition, which is necessary for defect formation is the condition of cavitation:

$$P_v > P + P_{\text{out}} \tag{28}$$

where the internal pressure P was calculated through (22). The vapour pressure was taken in the form

$$P_v = P_1^0 a \tag{29}$$

The vapour pressure of pure LMWC P_1^0 is derived from the Clausius–Clapeyron relationship

$$\ln P_1^0 = -\frac{\Delta H_{\text{vap}}}{RT} + \text{i} \tag{30}$$

where ΔH_{vap} is the enthalpy of vaporization, i is a constant. The Flory–Huggins relation for the activity of LMWC is

$$a = \varepsilon_1 \exp(\varepsilon_2 + \chi\varepsilon_2^2) \tag{31}$$

where ε_1, ε_2 are the volume fractions of LMWC and HMWC, respectively. The numerical values of all parameters are given in the Appendix.

If inequality (28) is valid and binder is in the superheated state the internal fluctuations of porosity should occur. After porosity formation the local pressure in the binder becomes

$$P = P_v - (\theta - 1)P_c \tag{32}$$

where P_c is the capillary pressure and θ is the porosity formed by cavitation. P_c is given by

$$P_c = P_v - P_l \tag{33}$$

where P_l is the pressure in the liquid phase and (32) is the result of the representation of the pressure as the volume average parameter.

$$P = (1-\theta)P_l + \theta P_v \tag{34}$$

Local porosity is small and cannot grow if it is not accompanied by the deformation of powder skeleton. Note that binder remains in the superheated state even after formation of cavities.[18] The condition for irreversible deformation (27) can be rewritten in the form

$$\varphi = \frac{\tau_T}{(P_{\text{out}} - P_v + P_T)\tan\varphi} > 1 \tag{35}$$

where $P_T - P_v$ corresponds to I_1 in (27), P_0 equals P_{out} and P_T, τ_T are invariants of the stresses, which occur due to non-uniform shrinkage of the powder compact. In our case the contribution of the capillary pressure to the strength of the powder compact is negligible in comparison with other terms.

Parameter ϕ becomes large in two different cases: if non-uniformity of the shrinkage is considerable and τ_T is large or if the vapour pressure is large and denominator of (35) is small. The second case corresponds to the fracture criterion (25) and it describes the bloating in the volume of the powder compact. Cracking occurs if (35) becomes valid at the surface of the powder compact. Realization of the different fracture mechanisms depends on the elastic properties of the powder compact at high temperatures. The Frankel–Acrivos approach[12] gives for the effective shear elastic modulus the following approximation:

$$G = \frac{9}{8} G_P \frac{(\varepsilon_s/\varepsilon_{\max})^{\frac{1}{3}}}{1-(\varepsilon_s/\varepsilon_{\max})^{\frac{1}{3}}} \tag{36}$$

where $\varepsilon_{\max}$ is the maximum powder loading in the feedstock. According to (36) the importance of the cracking mechanism decreases with decrease of the shear modulus of the binder and powder volume concentration.

5 Results of the Modelling

In Refs 3 and 19 detailed numerical calculations were performed for the prediction of the vapour pressure in the mouldings and the onset of bloating according to (25). We shall concentrate on the prediction of surface cracking with the use of (35). The maximum value of ϕ at the surface of the powder compact was used as indicator of damage development

$$\phi_c = \max_s \phi \tag{37}$$

The computer modelling of thermal debinding was accomplished for straight cylinders with different aspect ratio and for slabs with the same aspect ratio in cross-section. The half of the cylinder and the quarter of the slab were meshed into 400 elements. The typical distribution of the parameter ϕ in the volume of the 3 mm diameter cylinder is given in Fig. 1. The maximum values of ϕ are reached in the middle of the lateral surface and butt ends of the cylinder.

Numerical modelling needs detailed specification of all physical parameters. The diffusion coefficient D, viscosity μ and degradation rate of polymer were taken from[3] where careful measurements for poly-alphamethylstyrene were carried out. All values of the variables used in the calculations are given in the Appendix.

Numerical modelling of transport processes gives opportunity for the calculations of weight loss during thermal debinding. In the present case the diffusion of LMWC is the main transport mechanism. The diffusion coefficient exponentially increases with temperature and outward LMWC transport does not decline during all initial stages of debinding in spite of the smoothing of concentration gradient with time. The weight loss curves for the 3 mm diameter rod (it is a cylinder with aspect ratio 1:7) are given in Fig. 2. It is clear from the picture that debinding with a higher heating rate is the least time-consuming, but the increase of heating rate is restricted by the damage to the workpiece.

The internal stresses and parameter ϕ_c in the workpiece are very sensitive to the rate of heating and dimensions of the part. In line with experimental investigations[3] the heating of the powder compact with poly-alphamethylstyrene binder from 230° to 330° was considered. The internal

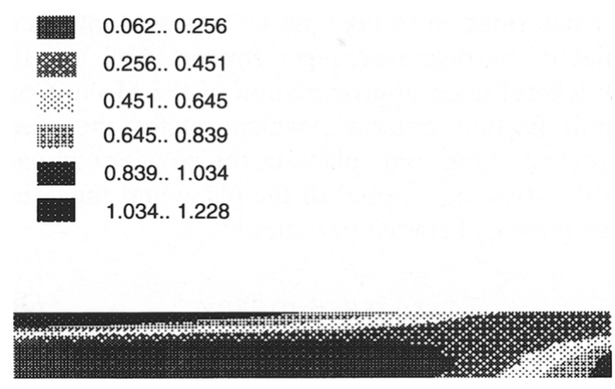

Fig. 1. Typical distribution of the fracture parameter ϕ in the volume of the rod during debinding. Heating rate 2°C h^{-1}, T=270°C.

elastic stresses were calculated and maximum value of ϕ was assessed. Parameter ϕ_c as a function of temperature for the different heating rates in the case of 3 mm diameter cylinder with the aspect ratio 1:7 is given in Fig. 3. Experiments in this case predict the critical heating rate between $1°\,h^{-1}$ and $2°\,h^{-1}$. Calculations give good agreement with experiments in spite of unknown real elastic properties of the powder compacts in the experiments. The parameter ϕ_c in the workpiece increases with the heating rate.

The level of the stresses is conditioned by the volume-to-surface ratio of the part. The increase of the cylinder dimensions intensifies the pressure build up. Figure 4 shows results for the parameter ϕ_c for cylinders with 3 mm and 5 mm diameters and equal heights at heating rates of $2°C\,h^{-1}$ and $0{\cdot}2°C\,h^{-1}$, respectively. The parameter ϕ_c is compared for 3 mm diameter cylinders with 1:7 aspect ratio and with height equal to the diameter in Fig. 5. It is important to note that if we decrease shear elastic modulus or increase friction angle to fit theoretical calculations for 3 mm diameter cylinders to experimental data, the theoretically predicted critical heating rates for 5 mm diameter cylinders fall into the experimental range (see Fig. 6).

Finite element modelling offers strong potentialities for the debinding imitation for parts of arbitrary shapes. The comparison of the critical heating rates for a 3 mm cylinder with the aspect ratio 1:7 and the slab with the same ratio of height

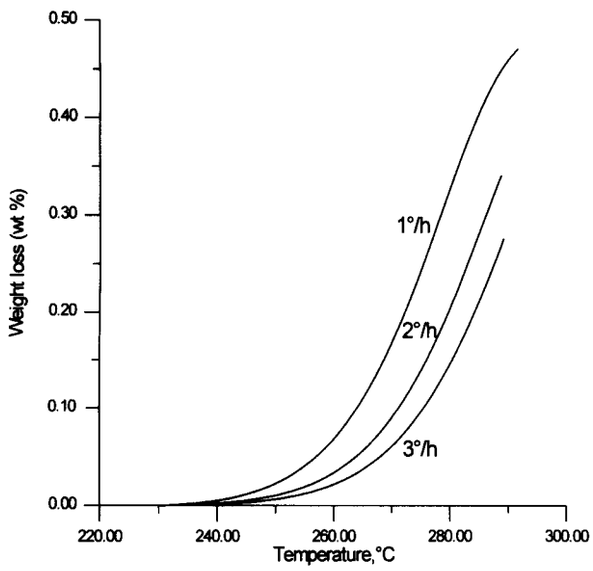

Fig. 2. Weight loss for 3 mm diameter rod.

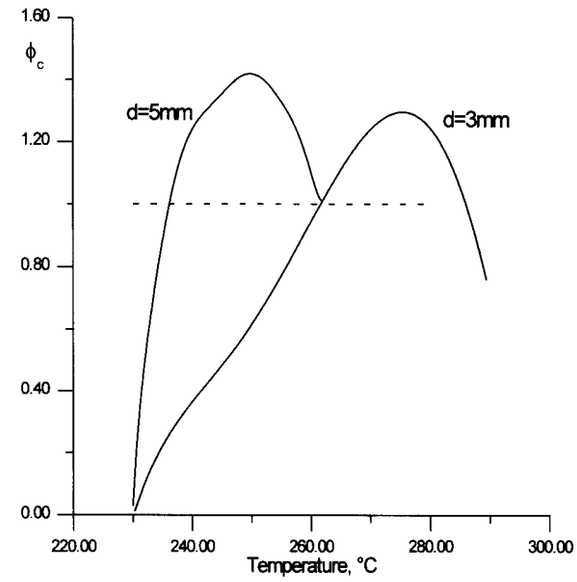

Fig. 4. Evolution of parameter ϕ_C during debinding of 5 mm diameter rod with heating rate $0{\cdot}2°C\,h^{-1}$ and 3 mm diameter rod with heating rate $2°C\,h^{-1}$.

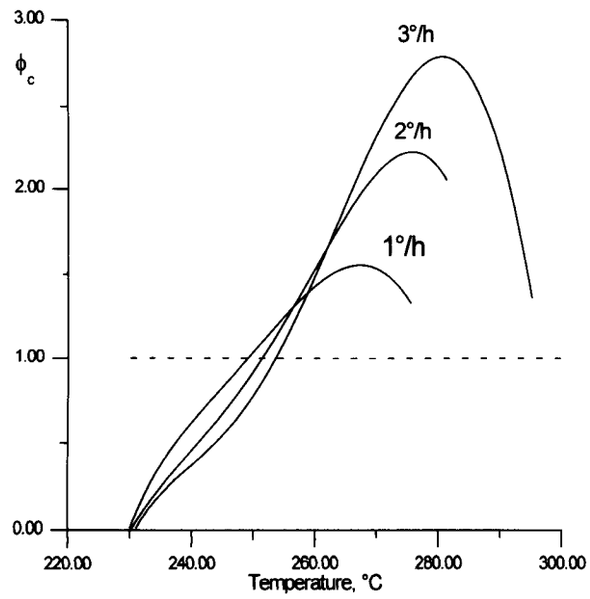

Fig. 3. Evolution of the parameter ϕ_C for different heating rates in the case of 3 mm diameter rod.

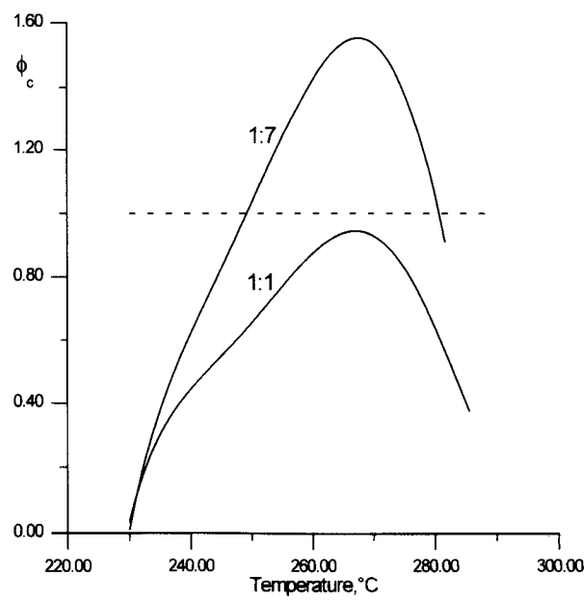

Fig. 5. Influence of the aspect ratio of 3 mm diameter cylinders on the evolution of the fracture parameter.

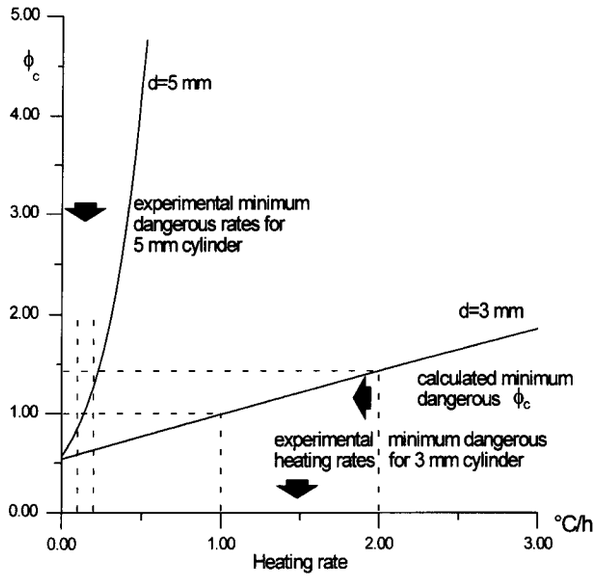

Fig. 6. Scheme of the comparison with experimental data.

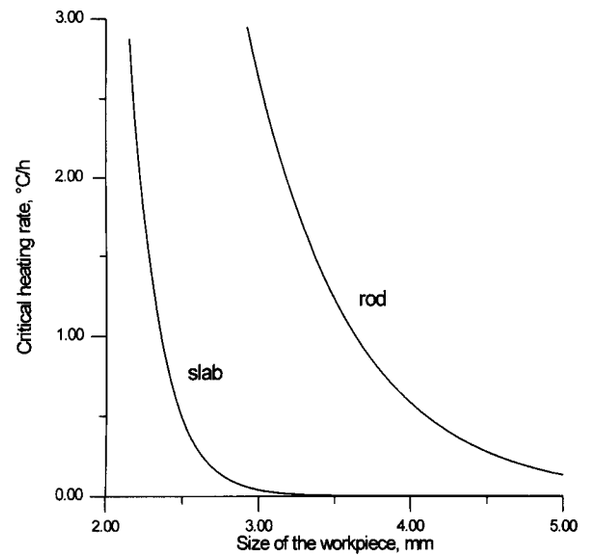

Fig. 7. Critical heating rates for the infinite slab and 3 mm diameter rod.

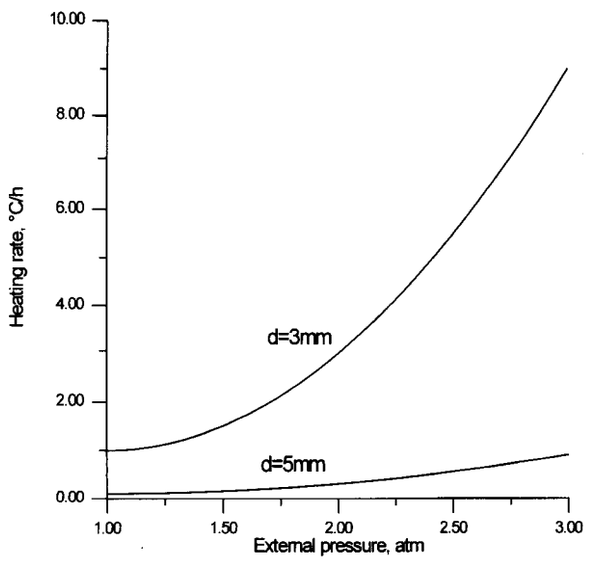

Fig. 8. Influence of the ambient pressure on the critical heating rate.

to thickness are given in Fig. 7. The results of Fig. 7 are similar to the results of Ref 19, but the explanation of the effect is different.

An important feature of the debinding process is its sensitivity to the external pressure. According to criterion (35) the strength of the powder compact must increase with increasing external pressure. Experiments confirmed this conclusion in the pressure range between 0·1 and 0·6 MPa.[14] Theoretical results for the critical heating rates of 3 mm and 5 mm diameter rods are given in Fig. 8. As in the case of the utilization of the fracture criterion (25), condition (35) gives unreasonably high critical heating rates at pressure above 0·6 MPa. A possible explanation of such discrepancy is given in.[14] It may arise because of the assumption about infinite surface mass transfer coefficient and boundary condition.[15] At higher heating rates resistance to transfer LMWC across the boundary may become significant. In any case, theoretical and experimental results prove the effectiveness of overpressure for thermal debinding.

6 Conclusions

The present model of the coupled deformational and transport processes during the thermal debinding stage of the injection moulding process allows prediction of the weight loss and internal stresses in the powder compact during debinding. It gives strong potentialities for the optimization of binder removal by the choice of safe heating regime with maximum weight loss. The model can be treated as a combination of the approaches of the theory of drying and theory of debinding. It gives plausible explanation to the existing experimental observations and creates some basis for necessary future experiments about damage accumulation during debinding or drying.

References

1. Barone, M. R. and Ulicny, J. C., Liquid-phase transport during removal of organic binders in injection-molded ceramics. *J. Am. Ceram. Soc.*, 1990, **73**, 3323–3333.
2. Angermann, H. H. and Van Der Biest, O., Low temperature debinding kinetics of two-component model system. *Int. J. Powd. Met.*, 1993, **29**, 239–250.
3. Evans, J. R. G., Edirisinghe, M. J., Wright, J. K. and Crank, J., On the removal of organic vehicle from moulded ceramic bodies. *Proc. R. Soc. London, A*, 1991, **432**, 321–340.
4. Cussler, E. L., *Multicomponent Diffusion.* Elsevier, Amsterdam, 1976, pp. 35–38.
5. Haase, R., *Thermodynamik der Irreversiblen Prozesse.* Dr Dietrih Steinkopff verlag, Darmstadt, 1963.
6. Mazurov, P. A., Variational approach in theory of filtration consolidation and two-phase filtration. *Appl. Math. Mech.*, 1992, **56**, 77–86.

7. German, R. M., Porosity and particle size effect on the gas flow characteristics of porous metals. *Powd. Tech.*, 1981, **30**, 81–86.
8. Timoshenko, S. and Goodier, J. N., *Theory of Elasticity*, McGraw Hill, New York, 1971.
9. Van Krevelen, D. W., *Properties of Polymers*. Van Krevelen, D. W. and Moftyzer, P. J., eds. Elsevier, Amsterdam, 1976.
10. Tsai, D.-S., Pressure buildup and internal stresses during binder burnout: numerical analysis. *AIChE Journ.*, 1991, **37**, 547–554.
11. Vrentas, J. S. and Duda, J. L., Diffusion in polymer-solvent systems II. A predictive theory for the dependence of diffusion coefficients on temperature, concentration and molecular weight. *J. Polym. Sci.*, 1977, **15**, 417–439.
12. Frankel, N. A and Acrivos, A., On the viscosity of a concentrated suspension of solid spheres. *Chem. Eng. Sci.*, 1967, **22**, 847–853.
13. German, R. M., *Particle Packing Characteristics*. MPIF, Princeton, 1989.
14. Hammond, P. D. and Evans, J. R. G., Thermolytic debinding of ceramic mouldings using overpressure. *Chem. Eng. Sci.*, 1995, **50**, 3187–3200.
15. Scherer, G. W., Theory of drying. *J. Am. Ceram. Soc.*, 1990, **73**, 3–14.
16. Lambe, T. W. and Whitman, R. V., *Soil Mechanics*. John Wiley, New York, 1969.
17. Hockey, B. J. and Wiederhorn, S. M., Effect of microstructure on the creep of siliconized silicon carbide. *J. Amer. Ceram. Soc.*, 1992, **75**, 1822–1830.
18. Udell, K. S. and Fitch, J. S., Heat and mass transfer in capillary porous media considering evaporation, condensation and non-condensible gas effects. *Am. Soc. Mech. Eng. Heat. Transfer Div.*, 1985, **46**, 103–110.
19. Matar, S. A., Edirisinghe, M. J., Evans, J. R. G. and Twizell, E. H., Diffusion of degradation products in ceramic mouldings during pyrolysis: effect of geometry. *J. Amer. Ceram. Soc.*, 1996, **79**, 749–755.

APPENDIX

Diffusion constant:[3]

$$D_L = D_{01}(1-\varepsilon_1)^2(1-2\chi\varepsilon_1)\exp\left\{-(y_1V_1(0)+y_2\zeta V_2(0))/(V_f/\omega)\right\}$$

$$D_{01} = D_0\exp(-E/RT)$$

$$V_f/\omega = (K_{11}/\omega)y_1\left[(c_2)_1 + T - (T_g)_1\right] + (K_{12}/\omega)y_2\left[(c_2)_2 + T - (T_g)_2\right]$$

$$V_1(0) = 8{\cdot}686\times10^{-4}\ \mathrm{m^3\ kg^{-1}}$$

$$V_2(0) = 7{\cdot}975\times10^{-4}\ \mathrm{m^3\ kg^{-1}}$$

$$K_{11}/\omega = 1{\cdot}756\times10^{-6}\ \frac{\mathrm{m^3}}{\mathrm{kgK}}$$

$$K_{12}/\omega = 5{\cdot}127\times10^{-7}\ \frac{\mathrm{m^3}}{\mathrm{kgK}}$$

$$(c_2)_2 = 49{\cdot}3K$$

$$(c_2)_1 = 13{\cdot}27K$$

$$E = 38370\ \mathrm{J\ mol^{-1}}$$

$$(T_g)_1 = 120\mathrm{K}$$

$$(T_g)_2 = 442\mathrm{K}$$

$$D_0 = 6{\cdot}92\times10^{-4}\ \mathrm{m^2\ s^{-1}}$$

$$\zeta = 0{\cdot}54$$

Viscosity of the polymer:[3]

$$\eta = \exp(A + B/(T - T_0))$$

$$A = 2{\cdot}303(12 - (c_2)_2)$$

$$B = 2{\cdot}303(c_1)_2(c_2)_2$$

$$T_0 = T_g - (c_2)_2.$$

Kinetics of the polymer degradation:[3]

$$\frac{\mathrm{d}y_2}{\mathrm{d}t} = -Ay_2$$

$$A = A_0\exp(-E/RT)$$

$$A_0 = 1{\cdot}67\times10^{16}\ \mathrm{s^{-1}}$$

$$E = 222000\ \mathrm{J\ mol^{-1}}.$$

Average diameter of the powder particles: $\mathrm{d} = 10\,\mu\mathrm{m}$.

Elastic properties of the binder:[9]

$$K_p = 2{\cdot}4\times10^9\ \mathrm{Pa}$$

$$G_P = 10^4\ \mathrm{Pa}.$$

Lame constants of the skeleton:[10]

$$\lambda = 116{\cdot}9\times10^5\ \mathrm{Pa}$$

$$G = 77{\cdot}9\times10^5\ \mathrm{Pa}.$$

Enthalpy of vaporization[3] $\Delta H_{\mathrm{vap}} = 38940\ \mathrm{J\ mol^{-1}}$. Constant in Clausius–Clapeyron equation[3] $\mathrm{i} = 22{\cdot}255$. Surface tension $\sigma = 0{\cdot}0407\ \mathrm{N\ m^{-1}}$.